Solid State Communications, Vol. 88, Nos. 11/12, pp. 871-875, 1993.
Printed in Great Britain.

0038-1098/93$6.00+.00
Pergamon Press Ltd

THE ELECTRONIC STRUCTURE OF h.c.p. YTTERBIUM

O. Jepson

Laboratory for Electrophysics, Technical University, Lyngby, Denmark

and

O.K. Anderson

Physics Laboratory I, H.C. Ørsted Institute, University of Copenhagen

(*Received* 4 *August* 1971 *by N.I. Meyer*)

The energy bands and Fermi surface of h.c.p. Ytterbium have been calculated by the relativistic APW method. The results are in good agreement with recent dHvA data. A new procedure for the calculation of cross-sectional areas and other geometrical properties of the Fermi surface is presented.

THE DIVALENT, rare earth metal Ytterbium exhibits several phase transitions.[1,2] Johansen and Mackintosh [3] calculated the energy bands for the f.c.c. phase and attempted to explain the pressure induced metal–semiconductor and subsequent f.c.c.–b.c.c. transition by *d*-band effects. However, they made only qualitative arguments since they found that the Fermi energy at normal pressure lay in an *sp-d* hybridization gap, although dHvA measurements had demonstrated the existence of a Fermi surface.[4] Recently it was discovered that, below room temperature and at normal pressure, the h.c.p. rather than the f.c.c. phase is stable,[2,5] and accordingly the dHvA results[4] applied to the former.[6] In this letter we present the h.c.p. energy bands and Fermi surface and show the latter to be in good agreement with the dHvA data of Tanuma *et al.*[6]

The calculation was performed *a priori* using the relativistic augmented-plane-wave method[7] with a muffin-tin potential constructed from self-consistent Dirac–Slater atomic wavefunctions[8] in the configuration $4f^{14}5d6s$. The Slater $\rho^{1/3}$ approximation was used for the exchange and good convergence was obtained with a basis of 42 APW's. The lattice constants adopted were $a = 3.911$ Å and $c = 6.403$ Å measured at 540°K.[9] Two sets of more recent values[2,5] have been determined at 300°K, but they differ from each other, and from the above values, by about 1 per cent.

The eigenvalues[10] were calculated in the irreducible zone on meshes, consisting typically of some hundred points around each sheet of Fermi surface, and the constant energy surfaces were found by linear interpolation. The volumes and cross-sectional areas were found as the sum of contributions from tetrahedral microzones determined by the mesh. Analytical expressions for these contributions may be found in Table 1. Since this procedure treats cross-sectional areas it is an extension of the method of Gilat and Raubenheimer.[11] Further it uses tetrahedra of arbitrary shapes, rather than boxes, and is therefore simpler and more accurate: All quantities are expressed in terms of the tetrahedral volume and the computed eigenvalues at the corners. The shapes of the tetrahedra are immaterial and they need not be congruent;

Previously published in: *Solid State Commun.* Vol. 9, No. 20, pp. 1763-1767 (1971)

Table 1. Linear interpolation of eigenvalues $\epsilon(k)$ in a tetrahedral microzone

	$n(\epsilon^a\epsilon^b\epsilon^c\epsilon^d, E; V)$	$N(\epsilon^a\epsilon^b\epsilon^c\epsilon^d, E; V)$	$A(\epsilon^a\epsilon^b\epsilon^c\epsilon^d, E; \phi^a\phi^b\phi^c\phi^d, F; V)$
$\epsilon_1 \leqslant E \leqslant \epsilon_2$	$V\Delta_1^3/\Delta_{21}\Delta_{31}\Delta_{41}$	$3V\Delta_1^2/\Delta_{21}\Delta_{31}\Delta_{41}$	$N[\phi^{11}\phi^{12}\phi^{13}\phi^{14}, F;$ $n(\epsilon^a\epsilon^b\epsilon^c\epsilon^d, E; V)]$
$\epsilon_2 \leqslant E \leqslant \epsilon_3$	$V\Delta^{-2}[\Delta_{31}\Delta_{41} + \Delta_{32}\Delta_{42} + \Delta\Delta_m$ $(3 - \Delta^2\Delta_m^2/\Delta_{31}\Delta_{41}\Delta_{32}\Delta_{42})]$	$3V\Delta^{-1}[1 - \Delta^2\Delta_m^2/$ $\Delta_{31}\Delta_{41}\Delta_{32}\Delta_{42}]$	$N(\phi^{11}\phi^{13}\phi^{14}\phi^{24}, F;$ $-V\Delta_1^2\Delta_4/\Delta_{31}\Delta_{41}\Delta_{42}) +$ $N(\phi^{22}\phi^{23}\phi^{24}\phi^{13}, F;$ $-V\Delta_2^2\Delta_3/\Delta_{31}\Delta_{32}\Delta_{42}) +$ $N(\phi^{11}\phi^{22}\phi^{13}\phi^{24}, F;$ $V\Delta_2\Delta_1/\Delta_{42}\Delta_{31})$
$\epsilon_3 \leqslant E \leqslant \epsilon_4$	$V[1 + \Delta_4^3/\Delta_{41}\Delta_{42}\Delta_{43}]$	$3V\Delta_4^2/\Delta_{41}\Delta_{42}\Delta_{43}$	$N(\phi^{11}\phi^{22}\phi^{33}\phi^{44}, F; V) -$ $N(\phi^{41}\phi^{42}\phi^{43}\phi^{44}, F;$ $-V\Delta_4^3/\Delta_{41}\Delta_{42}\Delta_{43})$
$\epsilon_4 \leqslant E$	V	0	$N(\phi^{11}\phi^{22}\phi^{33}\phi^{44}, F; V)$

Formula for the number of states n, density of states N, and cross sectional area A. The quantities in this Table are defined as follows:

$\epsilon(\underline{k}) = E$: Constant energy surface. V: Volume of tetrahedral microzone *abcd*. ϵ^i: Eigenvalue at i'th corner of *abcd*. $n(\epsilon^a\epsilon^b\epsilon^c\epsilon^d, E; V)$: Volume of that part of *abcd* in which the energy is less than E. $N(\epsilon^a\epsilon^b\epsilon^c\epsilon^d, E; V) = dn/dE$. ϵ_i: Subscripted quantities are superscripted quantities ϵ^i ordered according to magnitude: $\epsilon_1 \leqslant \epsilon_2 \leqslant \epsilon_3 \leqslant \epsilon_4$. An exception is $\epsilon_m \equiv (\epsilon_4\epsilon_3 - \epsilon_2\epsilon_1)/\Delta$, with $\Delta \equiv \epsilon_4 + \epsilon_3 - \epsilon_2 - \epsilon_1$. $\Delta_i \equiv E - \epsilon_i$. $\Delta_{ij} \equiv \epsilon_i - \epsilon_j$. $\phi(\underline{k}) = F$: Plane of cross section. ϕ^i: Value of function $\phi(\underline{k}) \equiv \hat{u}\cdot\underline{k}$ at i'th corner of *abcd*. $\hat{u}$: Unit vector along the magnetic field. F: Distance from the origin to plane of cross section. ϕ^{ii}: Value of $\phi(\underline{k})$ at that corner, where the eigenvalue is ϵ_i. $\phi^{ij} = \phi^{ji} \equiv [\phi^{ij}(E - \epsilon_i) - \phi^{ii}(E - \epsilon_j)]/(\epsilon_j - \epsilon_i)$: Value of $\phi(\underline{k})$ on the ij-edge of *abcd* and on the constant energy surface.

$A(\epsilon^a\epsilon^b\epsilon^c\epsilon^d, E; \phi^a\phi^b\phi^c\phi^d, F; V)$: Area of that part of the plane $\phi(\underline{k}) = F$, lying in *abcd*, where the energy is less than E. Subscripted quantities and Δ's are defined for the ϕ's as for the ϵ's.

moreover any irreducible zone can be divided into tetrahedra. The absolute error of a cross-sectional area due to the linear interpolation is usually less than the area of the largest tetrahedral face and in the present calculation the relative error was always less than 10^{-3}.

The Fermi level was determined by the requirement that the volumes of electron and hole surfaces should be equal. The *extremal* areas were found by locating the zeros of dA/dF, the analytical expression of which is easily found from the formulae of Table 1, and the cyclotron masses were found by numerical differentiation of extremal areas with respect to E.

The relevant energy bands are shown in Fig. 1. The narrow, spin-orbit split 4*f* bands occurring at 0.18 Ry and 0.29 Ry below the Fermi level are not shown. The Fermi energy is 342.8 mRy above the bottom of the free-electron-like 6*sp* band and the 5*d* band begins immediately below E_F. This band structure for Yb is very similar to those calculated for trivalent, h.c.p. rare earths Gd, Dy, Er, and Lu.[12] Their state densities as functions of energy all show a pronounced dip, although they do not fall to zero, at a concentration of two electrons per atom. For divalent Yb the Fermi level falls in this depression, caused by the *sp-d* hybridization, and the Fermi surface holds only 0.01557 electrons and the same number of holes; however, the state density of 11.12 states/(atom·Ry) is not particularly small. The third, predominantly *d*-like band of Yb is far more flat than those of the trivalent rare earths. Therefore the Fermi level lies just at the onset of a very steep peak in the density of states. This might provide a mechanism for the h.c.p.–f.c.c. transition.

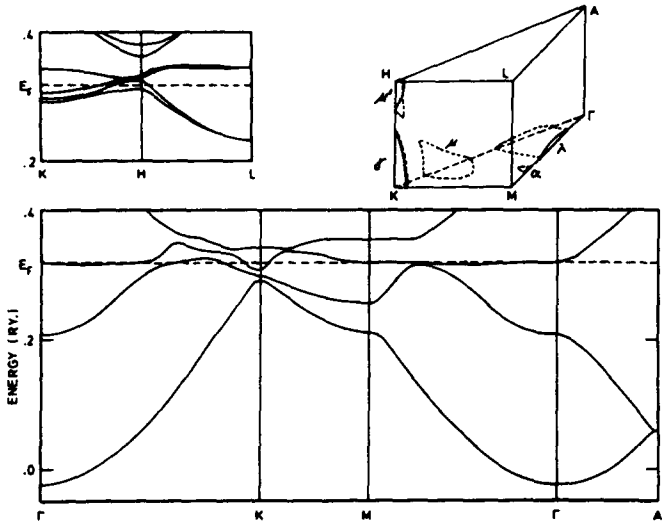

FIG. 1. Energy bands and Fermi surface sections for Yb.

Table 2. Theoretical Fermi surface parameters.

Band	Surface	Number of states [states/atom]	Density of states [states/(atom·Ry)]	Cyclotron masses $[m/m_0]$
2	μ'	−0.00089	0.24	[0001] 0.076 [10$\bar{1}$0] 0.36
2	μ	−0.01468	3.44	[0001] 1.14 [10$\bar{1}$0] 0.90 0.51
3	α	0.00022	0.67	[0001] 0.96 [10$\bar{1}$0] 0.28 0.39
3	γ	0.00280	0.49	[0001] 0.14 [10$\bar{1}$0] 0.53
3	λ	0.01255	6.28	[0001] 9.3 5.8 [10$\bar{1}$0] 0.87 1.71

The Fermi surface consists of two second band hole surfaces μ' and μ, and three third band electron surfaces α, γ, and λ.[13] The two former are the reminiscence of the Monster of the free-electron model, but the necks and the waists have disappeared, and thereby the possibility of open orbits. Of the electron pockets, γ corresponds to the Cigar and γ has a topology like the Lens, although with a hole in the middle. But γ is almost purely *d*-like, and so is α, which has no equivalent in the free-electron model. The partial state densities and volumes are given in Table 2.

Comparison of the total density of states with the electronic specific heat data of Lounasmaa[14] and of Bucher *et al.*[2] yield enhancement factors of 1.50 and 1.71 respectively.

The theoretical extremal areas, or dHvA frequencies, have been compared with the experimental data[6] in Fig. 2. Our calculation associates the low frequency branches with the electron pocket α rather than with hyperboloidal sections of the Monster. This we have further checked by lowering the Fermi energy artificially until μ' and μ become connected by a neck of

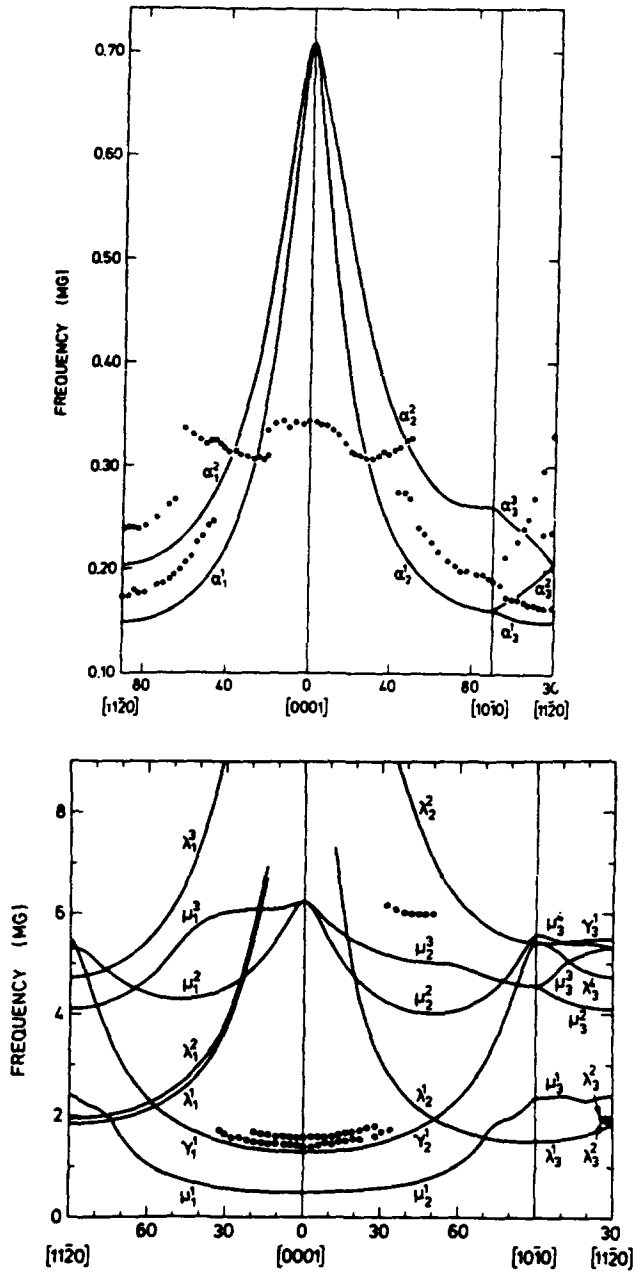

FIG. 2. Theoretical (full line) and experimental [6] (dots) dHvA frequencies in mega gauss for h.c.p. Yb. (a) low frequencies, (b) high frequencies.

the proper size; then, however, the angular variation of the deduced dHvA frequencies disagrees with the experimental results. The experimental data around 0.30 MG [6] may well be accounted for by beats between different branches. The theoretical μ-frequencies are too small; however, for such tiny sheets of Fermi surface the *relative* discrepancy between measured and calculated extremal areas is expected to be large and the good agreement for the angular variations is more significant. Using the cyclotron masses from Table 2 as described in reference 15 plus an estimate of the role of *sp-d* hybridization on the Fermi surface, we find

that a lowering of the *d*-band of the order of 10 mRy relative to the *sp*-band will bring all theoretical frequencies in agreement with the experimental values. This shift would also reduce the, otherwise rather high, specific heat enhancement factor. The small inaccuracy in the position of the bands could be accounted for by the uncertainty in the lattice constants alone, or by a very small inaccuracy in the potential.

Further results of this calculation will be presented elsewhere.

Acknowledgements – We are grateful to Professor A.R. Mackintosh for drawing our attention to this problem, and we have benefitted from the use of the facilities of the Northern Europe University Computing center.

REFERENCES

1. MCWHAN, D.B., RICE T.M. and SCHMIDT P.H., *Phys. Rev.* **177**, 1063 (1969).
2. BUCHER E., SCHMIDT P.H., JAYARAMAN A., ANDRES K., MAITA J.P., NASSAU K. and DERNIER P.D., *Phys. Rev.* **B2**, 3911 (1970).
3. JOHANSEN G. and MACKINTOSH A.R., *Solid State Commun.* **8**, 121 (1970).
4. TANUMA S., ISHIZAWA Y., NAGASAWA H. and SUGAWARA T., *Phys. Lett.* **25A**, 669 (1967).
5. KAYSER F.X., *Phys. Rev. Lett.* **25**, 662 (1970).
6. TANUMA S., DATARS W.R., DOI H. and DUNSWORTH A., *Solid State Commun.* **8**, 1107 (1970).
7. LOUCKS T.L., *Augmented Plane Wave Method*, Benjamin, New York (1967).
8. LIBERMAN D., WABER J.T. and CROMER D.T., *Phys. Rev.* **137**, A27 (1965).
   We are grateful to Dr. Cromer for supplying us with the atomic charge densities on which these calculations are based.
9. SPEDDING F.H., HANAK J.J. and DAANE A.H., *J. Less-Common Metals*, **3**, 110 (1961).
10. In the present calculation the APW determinants at energy E, rather than the eigenvalues, were used in the linear interpolation scheme.
11. GILAT G. and RAUBENHEIMER L.J., *Phys. Rev.* **144**, 390 (1966), and *Phys. Rev.* **157**, 586 (1967).
12. KEETON S.C. and LOUCKS T.L., *Phys. Rev.* **168**, 672 (1968).
13. For the Fermi surface sheets equivalent to those of Mg we have used the notation of STARK, *Phys. Rev.* **162**, 589 (1967).
14. LOUNASMAA O.V., *Phys. Rev.* **129**, 2460 (1963). As remarked in reference 2 this result applies to the h.c.p. phase.
15. ANDERSEN O.K., *Phys. Rev.* **B2**, 897 (1970).

Energibänder und Fermi-Fläche hexagonales Ytterbium sind durch die relativistische APW-Methode berechnet worden. Unsere Ergebnisse stimmen mit den spätesten dHvA Zahlenwerte gut überein. Es wird ein neues Verfahren zu Berechnung von Querschnitte und andere Eigenschafte der Fermi-Fläche dargestellt.